NASA Contractor Report 3654

Preliminary Test Results of Electrical Charged Particle Generator for Application to Fog Dispersal

Walter Frost
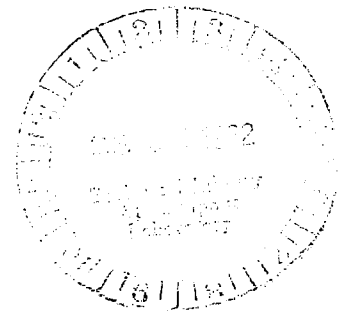
NASA

NASA Contractor Report 3654

Preliminary Test Results of Electrical Charged Particle Generator for Application to Fog Dispersal

Walter Frost
FWG Associates, Inc.
Tullahoma, Tennessee

NASA

National Aeronautics
and Space Administration

Scientific and Technical
Information Branch

1982

ACKNOWLEDGMENTS

TABLE OF CONTENTS

LIST OF ILLUSTRATIONS

DEFINITION OF SYMBOLS

A   Empirically determined constant

a   Empirically determined constant

E   Electric field (potential gradient)

E_{min} Minimum field at which discharge occurs

H   Height of needle above nozzle exit plane

I   Output current

M   Mach number

P   Pressure in nozzle

P_t Total pressure in plenum

P_* Pressure at nozzle throat

P_1 Nozzle plenum pressure

P_2 Pressure upstream of atomizer needle valve

P_3 Water supply tank pressure

RH   Relative humidity in atmosphere

V   Potential

V_0 Potential at which discharge occurs

$\dot{V}$ Liquid water volume flow rate

v   Velocity of ions

1.0 INTRODUCTION

A charged particle generator which produces a high-velocity jet of air and charged water droplets has been constructed and preliminary performance tests carried out. The generator accelerates air through a diverging/converging nozzle. A corona is generated either in the throat or at other positions along the nozzle. Water droplets formed in the nozzle are charged by the ions and/or electrons in the corona region and carried into the atmosphere by the kinetic energy of the air jet. The space charge in the vicinity of the nozzle is thus changed by continuous addition of charge and the atmospheric electric field in the vicinity of the generator is modified.

The proposed application of this prototype charged particle generator is to disperse fog by modifying its electric field structure. A strong electrical field will cause droplets either to coalesce (Mason 1971; Kolokolov and Lobodin 1974) and precipitate by gravitational effects or to follow the electric field lines to ground due to the natural or induced charges on the fog droplets. Although the microphysics by which the fog is dispersed is not known nor even whether fog can be dispersed in the natural atmosphere, a number of laboratory tests and some fields tests have suggested the mechanism is viable (Christensen and Frost 1980). Conflicting issues, however, have been raised. An exact analytical solution requires solving a highly coupled set of electro-hydrodynamic equations which at present are intractable even if all the microphysics could be modeled. Crude analyses which have been carried out have also raised conflicting issues. Christensen and Frost (1980) and Frost, et al. (1981) have reviewed these analyses and concluded that those analyses which support the electrical technique for fog dispersal are based on sounder physical and analytical principles. The next step in a systematic evaluation and proof of concept is to construct a charged particle generator to demonstrate that the estimated magnitudes of charge necessary to disperse fog (Chiang, et al. 1973;

Clark, et al. 1977) can be achieved practically and reliably. Thus, the purpose of this study was to build a charged particle generator fog dispersal unit and investigate the performance which can be achieved.

The results, although not having necessarily achieved the optimum in terms of charged particle generator performance, have shown that a relatively large amount of charge can be sprayed into the atmosphere with a charged particle generator of the prototype design. This is not overly surprising since a number of electrical gas dynamic systems have been built for power generation and other applications (Chiang, et al. 1973; Clark, et al. 1977; Marks and Kent 1979; Willke 1971).

The system developed and described in this report still requires some further modifications to answer a number of unresolved questions on performance of the system. However, the prototype generator which was constructed has been extremely useful in providing experience and "seat-of-the-pants" understanding of the various physical mechanisms involved.

This report describes the construction of the charged particle generator and the tests carried out to verify its potential capabilities. Section 2.0 describes the design and configuration of the charged particle generator, Section 3.0 presents the preliminary results achieved with testing the generator and interprets these results relative to the performance of the system, and Section 4.0 presents conclusions relative to modification of the existing unit and where future research should go relative to further development of the charged particle fog dispersal unit.

2.0 CHARGED PARTICLE GENERATOR

2.1 Experimental Apparatus

2.1.1 <u>General</u>

The general arrangement of the experimental apparatus is illustrated schematically in Figure 2.1. Complete details of the system design are provided in Collins, et al. (1981). The overall system will be referred to as the charged particle generator. The basic mechanism of the charged particle generator is one where high-pressure air is pumped through the primary air supply circuit to a converging/diverging nozzle. Water is injected into the primary airstream through a secondary water flow circuit. Droplets form in the nozzle due to condensation or upstream atomization. A corona region either in the throat or at positions further along the nozzle produces positive ions and electrons which charge the water droplets. The kinetic energy of the air accelerated through the nozzle carries the charged droplets into the atmosphere.

The charged jet of air creates a current source flowing into the atmosphere. This current is referred to in the following discussion as the current output as contrasted to the current supplied to the transformer which produces the high-voltage in the corona region. The various flow and electrical circuits making up the overall system are described individually in the following sections.

Figure 2.2 is a photograph of the overall system. The controls in the experimental system have been mounted at approximately shoulder height for ease of operation and of reading the instruments. This configuration of the system, although having exactly the same components as an operational system, is considerably taller. The operational system would be much more compact and lower to reduce obstruction height when located on an airfield.

3

90 psig Air
$(6.20 \times 10^5 \text{ N/m}^2)$

Hose Connector

Shut-Off Valve

Wilkerson Type A Filter
5 microns
F00-02-F00

Check Valve

Pressure Regulator
(Spraying Systems #11438-45)
with 0-100 psig $(6.89 \times 10^5 \text{ N/m}^2)$
Pressure Gauge (Spraying Systems #11438-73)

Pressure
Gage 0-100 psig
$(6.89 \times 10^5 \text{ N/m}^2)$
(Spraying Systems #11438-73)

Needle
Valve
Atomizer

Nozzle

Wilkerson Type C Filter
0.03 micron
M20-02-F00

Pressure Regulator
(Spraying Systems #11438-35)
with 0-100 psig $(6.89 \times 10^5 \text{ N/m}^2)$
Pressure Gage (Spraying Systems #11438-73)

Pressure
Gage
0-100 psig
$(6.89 \times 10^5 \text{ N/m}^2)$
(Spraying Systems
#11438-73)

Microammeters

20 kv DC
Variable
Power
Supply

4 Lindsay Model 15-HU Portable Air Compressor,
15 SCFM $(7.08 \times 10^{-3} \text{ m}^3/\text{s})$,
60-125 psig $(4.14 \times 10^5$
$- 8.62 \times 10^5 \text{ N/m}^2)$,
9 HP $(6.71 \times 10^3 \text{ W})$ Gasoline Engine

Shut-Off
Valve

0-100 psig $(6.89 \times 10^5 \text{ N/m}^2)$
Pressure Gage
(Spraying Systems #11438-73)

12-Gallon $(4.54 \times 10^{-2} \text{ m}^3)$
Water Tank

Liquid Strainer
(Spraying Systems #1/4 TW-B)

Rotameter
(Dwyer, Model VFB 82 SSV,
2-30 cc water/min)

NOTE: All plumbing is 1/4" (0.64 cm) galvanized steel pipe.

Figure 2.1   Schematic of charged particle generator.
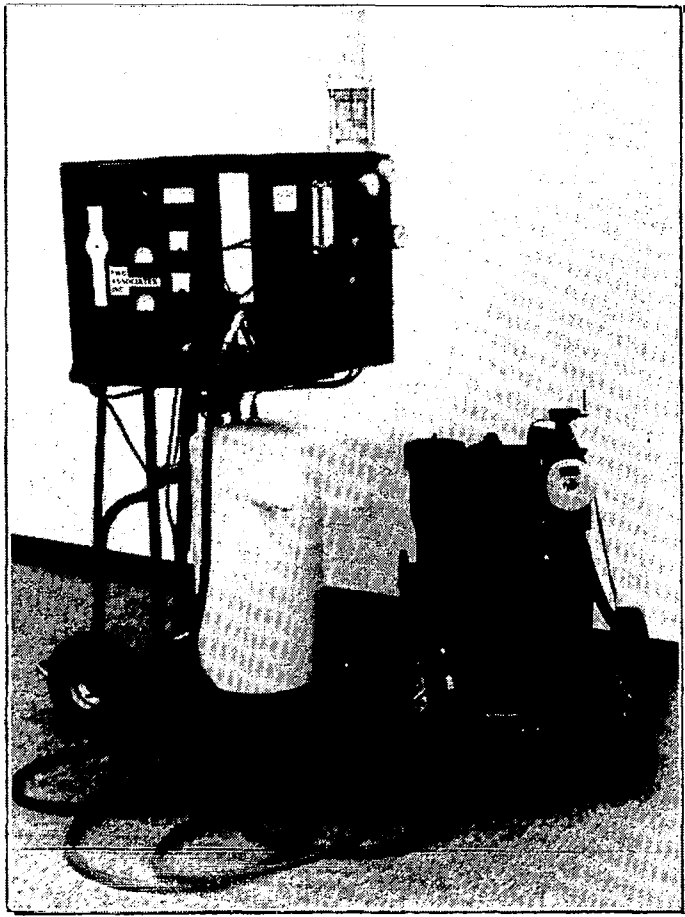
Figure 2.2 Photograph of overall fog dispersal system.

2.1.2 Air Supply Circuit

The air was supplied by a Lindsay Model 15-HU, 15 SCFM, 60 to 125 psig, gas-driven, portable air compressor. The compressor was set to operate at 125 psig. Air was accumulated in two compressor tanks of 2 ft^3 capacity each. These were found to be of insufficient size to serve effectively as accumulators and caused flow surges when the compressor regulator cut in. A method of eliminating or reducing these surges was not implemented during this study but will be in furture studies.

Air was supplied to the charged particle generator through a rubber hose connection. The air was initially filtered with a Wilkerson Type A, 5 µ filter for removing oil and particulate matter and a Wilkerson Type C, 0.03 µ filter for removing liquid water and finer

5

particulate matter. The filtered air was then split. One branch of the flow passed through a Spraying Systems #11438-35 regulator and was used to pressurize a 12-gallon water supply tank. The second branch passed through a Spraying Systems #11438-45 pressure regulator to the nozzle plenum chamber and thus through the nozzle throat to the atmosphere. Pressures in the plenum and in the water tank were measured with 0 to 100 psig pressure gages.

2.1.3 Nozzle

The nozzle was cast out of casting plastic (Plexiglas) with the dimensions shown in Figure 2.3. An attractor was positioned at 2 and 3 inches from the needle support. Needles were made of 0.0625-in diameter bicycle spokes with threaded ends. The spoke nuts were utilized to secure the needle to a machined brass support plate shown in Figure 2.4. The nozzle was then mounted to the Plexiglas support by four tie-down bolts as illustrated in Figure 2.5. With this tie-down arrangement, needles could be changed relatively quickly, although it was necessary to shut down the system. The needle position could not be adjusted externally during a run.

The nozzle was a converging/diverging nozzle originally designed for an exit Mach number of 1.35. The original design, however, called for a very thin corona needle [0.02 inch (0.5 mm)], which was found to vibrate under flow conditions. It was therefore necessary to go to a larger 0.0625-in diameter needle, which reduced the area of the throat region and thus changed the flow characteristics of the nozzle. With these new flow characteristics, supersonic flow was not achieved at the exit and shocks occurred somewhere in the diverging section of the nozzle.

The mass flow through the nozzle under choked conditions with the larger needle is still approximately 15 SCFM. No difficulties were encountered in achieving choked flow in the nozzle since a plenum pressure of 17 psia assured choked flow. It is not known, however, whether the effect of shocks in the nozzle appreciably degraded the performance of the system in terms of electrical current output.

NOTE: All dimensions in inches.
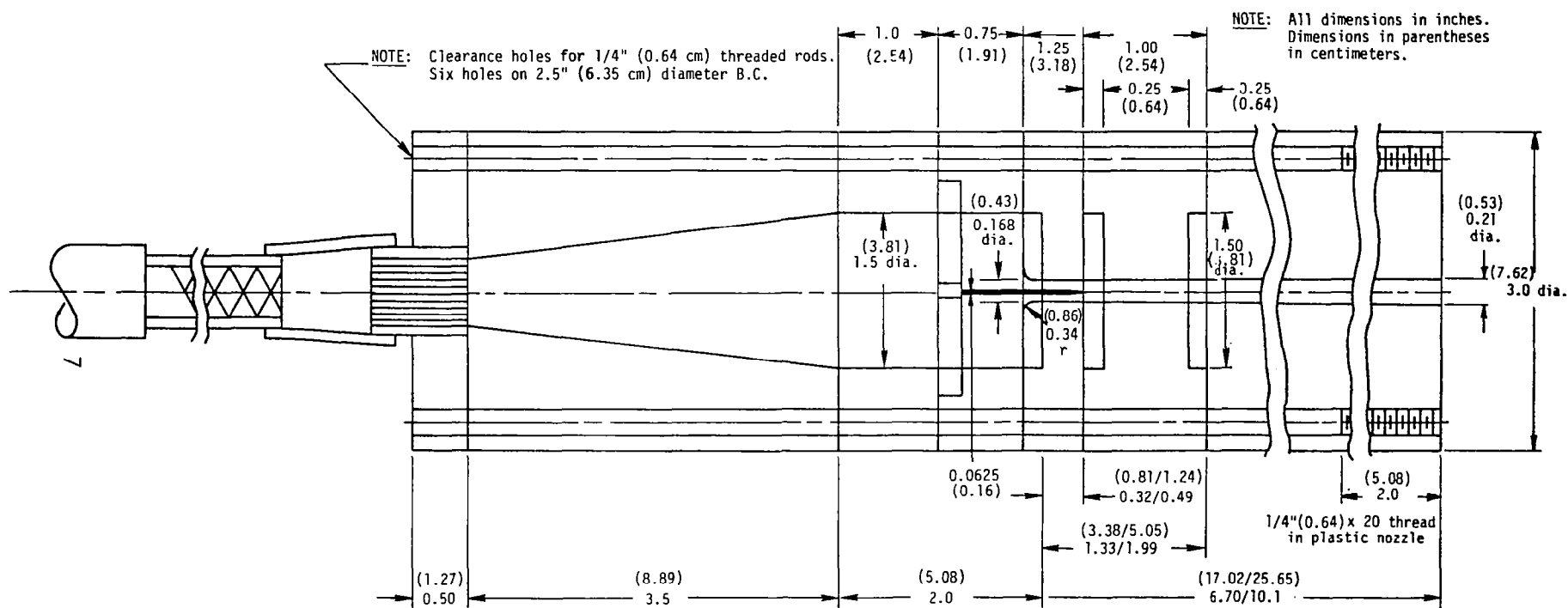Dimensions in parentheses
in centimeters.
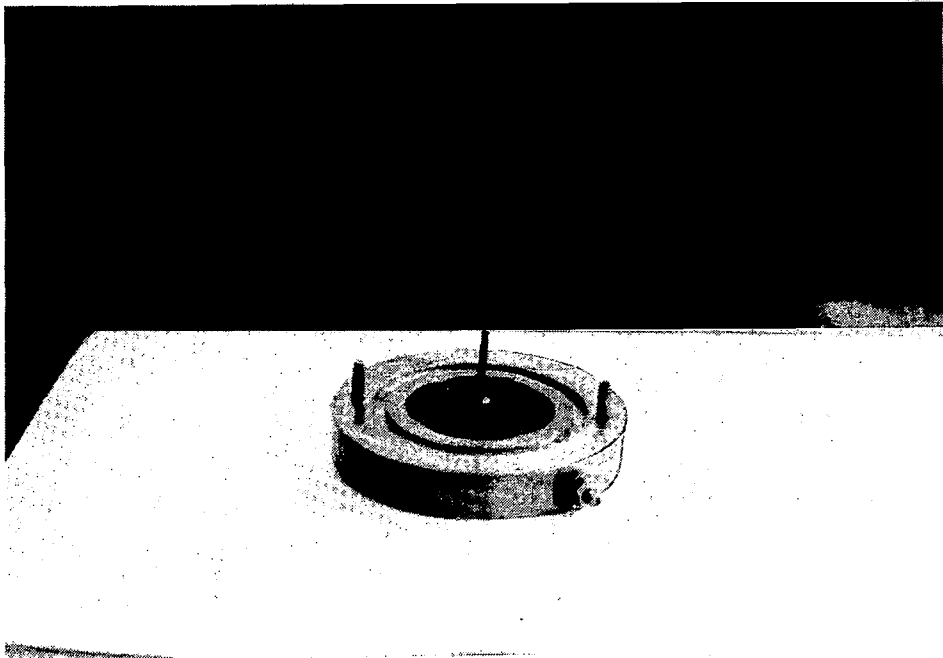
Figure 2.3 Dimensions of nozzle.

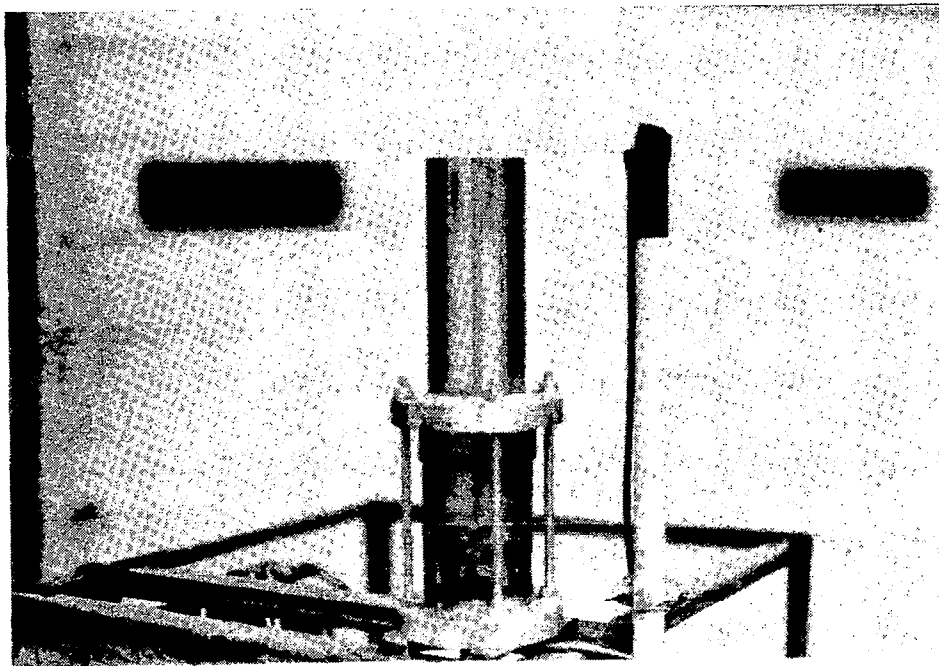Figure 2.4 Machined brass needle support plate and needle.

Figure 2.5 Cast Plexiglas nozzle and output current measuring needle arrangement.

2.1.4 Water Flow Circuit

Liquid water was supplied from a 12-gallon pressurized tank. The tank was pressurized with bleed flow from the primary air supply to the nozzle. Water flowed from the pressurized tank through a liquid strainer and then through a Dwyer Model VFB 82 SSV, 2 to 30 cc/min rotameter. The rotameter was equipped with a needle valve control, which was used to adjust the water flow rate for all runs. The water was injected into the airstream through an adjustable needle valve conceptually designed to atomize the flow. The concept was that the gap between the needle and its conical seat would be a measure of the size of droplets issuing into the airstream. However, experience showed that adjustment of the needle valve did not affect the performance of the system. Therefore, it was decided that the water sprayed into the air through the needle valve was fully evaporated regardless of the needle opening. Droplets were therefore assumed to have formed by recondensation in the nozzle consistent with the theory of Collins, et al. (1981) and Frost, et al. (1981). It should be noted that under optimum liquid flow conditions (approximately 6 cc/min), droplets were not visually observed leaving the nozzle; however, the presence of a current verified their existence. For example, when the water was totally turned off, the current output dropped to very low values (approximately 2 to 3 μa). In turn, at high flow rates (>8 cc/min), where liquid droplets shedding for the edges of the nozzle exits were plainly visible, the current again dropped off although not as significantly. At these high flow rates, water often collected on the outside needle or accumulated on top of the nozzle.

Experience also showed that it was extremely critical to clean the filters prior to each run. Other researchers (Chiang, et al. 1973; Collins, et al. 1981) have reported the importance of assuring clean water, in particular, removal of all oils. This was confirmed in the present experiments by the fact that if the filters were not cleaned prior to each run, performance of the system was significantly deteriorated.

2.1.5 Electrical Circuit

High voltage for generation of the corona was provided by a 20 kV DC transformer with a rheostat control to provide continuous voltages from 0 to 20,000 volts. The primary transformer circuit operates at 110 volts, which can be provided by a portable gasoline generator. To date, however, the primary power has been supplied by plugging into a standard public utility power supply. The primary circuit is connected to the transformer through a 0 to 10 ammeter, 0 to 150 volt voltmeter, and 1.5 amp circuit breaker switch. The ammeter and voltmeter are of very coarse scale. Consequently, the ammeter registers no current during normal testing conditions, whereas the voltmeter reads in the range of 10 to 40 volts depending on the rheostat setting.

The positive lead from the secondary side of the transformer runs through a 0 to 5 μa ammeter to the attractor. The negative lead runs through a 0 to 5 μa ammeter to the needle. The negative side is grounded. This connection results in a negative corona. As discussed later, the 0 to 5 μa ammeter in the circuit continually failed during testing.

2.1.6 Current Output Measurement Circuit

The current output of the charged particle generator was considered to be that measured with a needle arrangement as shown in Figures 2.5 and 2.6. The needle was supported on nonconducting PVC tubing, which could be positioned vertically by sliding up and down in its support. The needle could also be rotated to measure the current at different positions in the air jet as indicated in Figure 2.7. The needle point was grounded through a 0 to 100 μa ammeter. The ammeter measured the charge which flowed to ground through the needle.

This current measurement could not be converted directly to electric field but provided a measure of the performance of the charged particle generator. Until a better method of measuring the performance of the charged particle generator is developed, however, this setup provides a measure of the system performance that can be used for comparison between different system configurations and between different

10

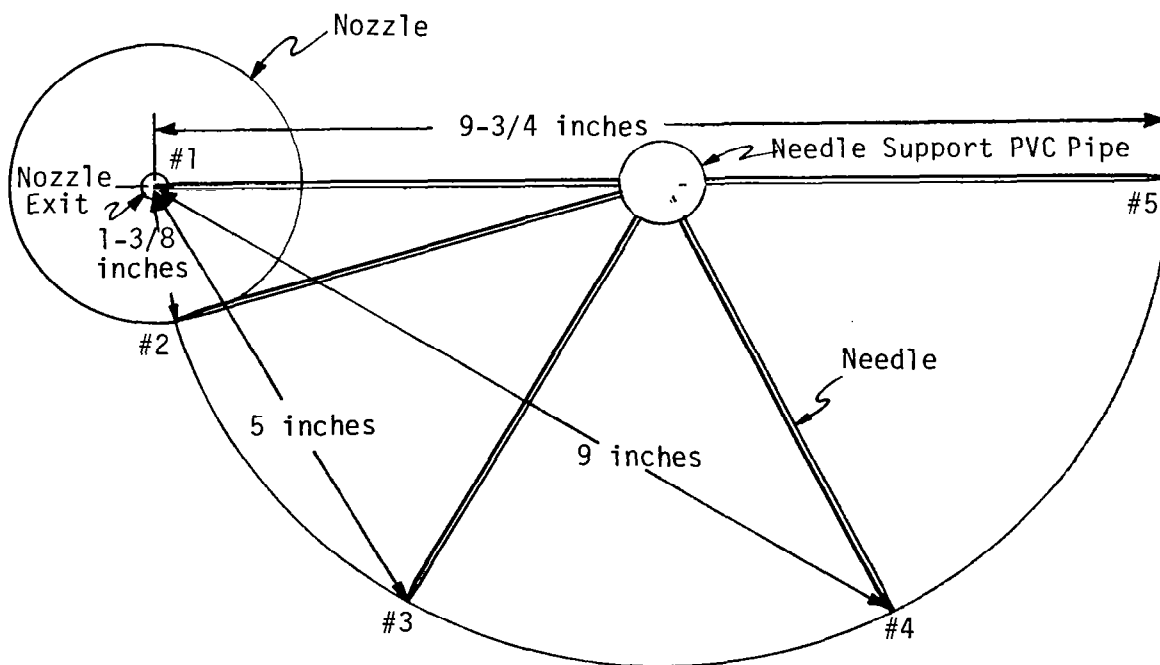Figure 2.6 Output current measurement needle.

Figure 2.7 Needle positions used in probing the charged jet.

settings of the system parameters (i.e., corona voltage, water flow, etc.).

The use of a point discharge current as a measurement of electric fields or potential gradient in the atmosphere is not new. Simpson and Scrase (1937) and Simpson and Robinson (1940) used this method with a balloon-borne instrument called an alti-electrograph. The alti-electrograph was designed merely to determine the direction of the vertical potential gradient in and near clouds, but it was later found that the magnitude as well as direction could be determined by relating the point discharge current to the potential gradient.

Measurements under laboratory conditions have shown that the relationship between the point discharge current and potential gradient has the form:

$$E = \left(\frac{I}{a} + E_{min}^2 \right)^{1/2} \tag{2.1}$$

where E is the potential gradient, I is the current, and a and E_{min} are constants for a given atmospheric condition. Measurements of atmospheric point discharge usually fit this type of equation. When measurements are made of the point discharge current in natural conditions, it is difficult to obtain accurate results because conditions are usually changing very rapidly; hence, there is always a wide scatter of results and thus agreement with any equation is poor. Whipple and Scrase (1936), however, report approximate values for a and E_{min}. They measured the point discharge current (I) and simultaneously the potential gradient (E) at the ground and fitted their results to Equation 2.1 finding for positive current through the point, E_{min} = 780 v/m and a = 8 x 10^{-14} a/(v/m)^2; for negative currents, E_{min} = 860 v/m and a = 10 x 10^{-14} a/(v/m)^2. E_{min} essentially represents the minimum field at which point discharge occurs (about 800 v/m at roughly 20 m).

The wind speed was shown to appreciably affect the natural point discharge current. Davis and Standring (1947) showed an increase of current with wind speed but no general equation was obtained. Chapman (1956), on general considerations, suggested that the correct form of

12

the relationship between point discharge current and potential should be:

$$I = a(V - V_0)v \qquad (2.2)$$

where v is the velocity with which ions are removed from the neighborhood of the point by the wind. When there is little wind, v is proportional to E since the ions are moved away by the field; and so

$$I = A(E - E_{min})E \quad . \qquad (2.3)$$

This equation is similar to that of Whipple and Scrase (1936). Other similar forms of this equation have been given, however, either the current goes to zero with zero wind or the coefficients for the equations cannot be generalized. In fact, the values of a and E_{min} presented earlier for Equation 2.1 are not general but are only representative values.

More recently, Harris (1969) made a crude measurement of the air-to-ground current at ground level using a 10 ft^2 (1 m^2) aluminum sheet well insulated and connected to ground through a 10^{10} ohm resistor. A capacitor was added to increase the time constant of the circuit to 10 minutes to minimize displacement current effects due mainly to the flowing of charged dust clouds above the measuring plate. (Note the experiment was an investigation of the effect of dust clouds on the atmospheric electric field.) This current measurement was simultaneously recorded with a six-bladed field mill. Figure 2.8, taken from this reference, shows a comparison of the measured electric field and the air/earth current. The measurements show that an increase in magnitude and a change of polarity in the air-to-ground current accompanies the field intensification and reversal. Although no accuracy is claimed for these measurements, the results can be used to demonstrate that the current measurement for the present experiment does represent at least qualitatively the electric field at the local point of the needle. Thus, it is believed the magnitude of the current measured through a grounded needle is a meaningful parameter to compare the charge particle generator performance under different experimental conditions.

13
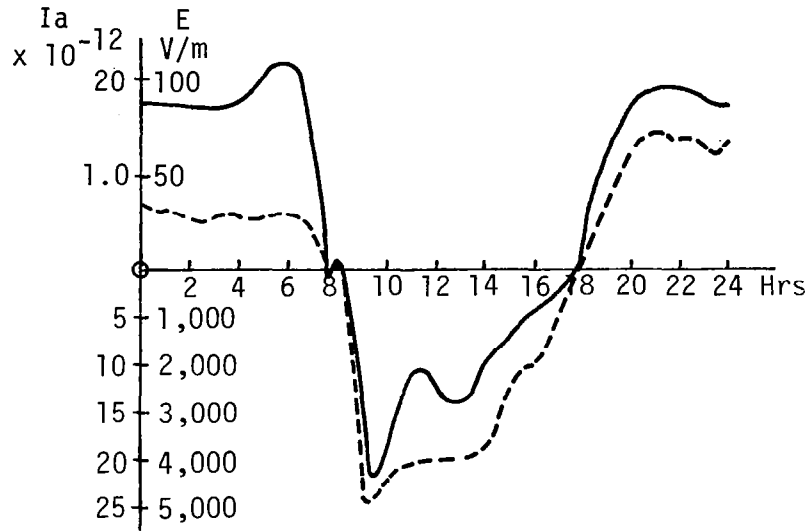
Figure 2.8 Air/earth discharge current and separately measured field
(Harris 1969).

2.2 Method of Testing

Tests were initiated by starting the compressor and allowing it
approximately 3 to 5 minutes to warm up. The unloader valve on the
compressor was then closed and the air tanks filled. The liquid water
tank was pressurized by adjusting regulator #1 in Figure 2.9.
Pressure gage P3 measures the tank pressure and was normally adjusted to
40 psig depending on the particular test to be carried out. Regulator
#2 was used to adjust the nozzle plenum pressure, P1, to typically
30 psig. This setting again depends on the test to be run. Gage P2
generally measured 32 to 33 psig once pressure P1 was set. The dif-
ference between P2 and P1 is a measure of the pressure drop across the
water flow needle valve. Once these pressures were set, they remained
essentially constant throughout the experiment. The accuracy with which
these gages could be read is approximately ±0.5 psig.

2.2.1 Water Flow

Depending on the particular experiment to be conducted, the test
procedure continued with either initiating the flow of water or, if
interest was in determining the current output without liquid water

Pressure Upstream of Atomizing
Needle Valve, P2

Nozzle
Plenum Pressure,
P1

NASA

Rotameter

Water Flow
Control Valve #3

Water Tank
Pressure, P3

Regulator #1

Regulator #2

15

Figure 2.9 Water flow control panel.

flow, switching on the electrical circuit. Assuming the former condition, liquid flow was introduced to the airstream by opening needle valve #3 below the rotameter. This valve was adjusted until th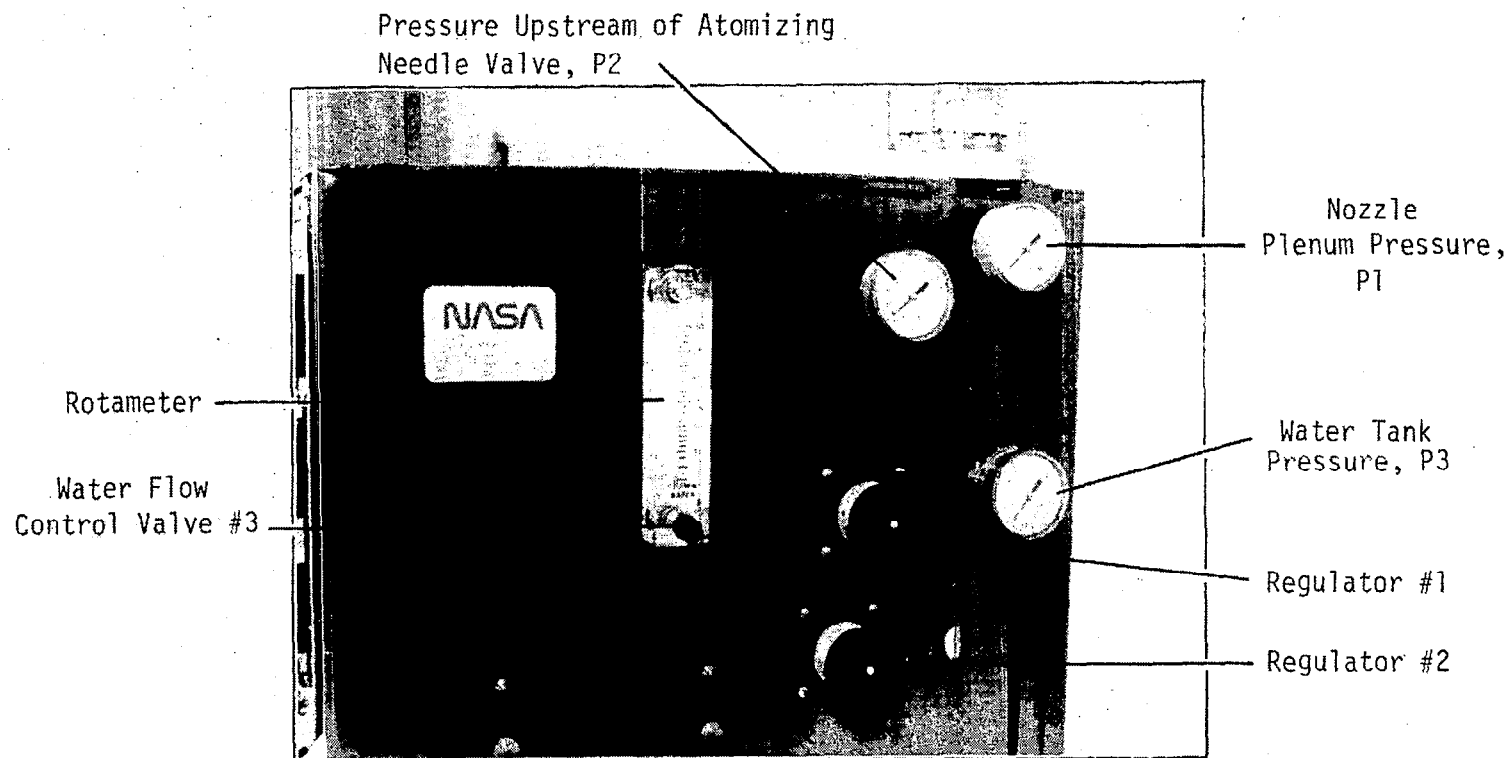e desired flow rate was established. The flow rate, however, continuously dropped off during all runs, and it was necessary to monitor the flow rate and adjust the valve routinely during each test. It is believed that as the liquid water was exhausted from the tank it allowed the back pressure to drop slightly and the flow to fall off with time. This could not be verified directly because pressure gage P3 always remained steady at the initial pressure setting. Occasionally, a surge in the water flow occurred which was associated with the regulator on the compressor kicking in or out as the storage tanks on the compressor became depleted or full.

Prior to a given test the humidity of the surrounding environment was measured with a sling psychrometer. This measurement was repeated periodically during a given run. It was anticipated that humidity will influence the output current measured because of its influence on the atmospheric conductivity. High atmospheric conductivity allows more current to leak to ground.

2.2.2 Power Supply

The power supply to the corona needle and attractor was initiated by switching on the primary power, switch #1, Figure 2.10. Switch #2, Figure 2.10, provided a ground through a 20 megohm resistance to discharge any residual voltage in the transformer upon completion of a test. It was necessary to assure that switch #2 was open before throwing switch #1. Rheostat #3, Figure 2.10, was then adjusted to obtain the desired voltage. Measurement of voltage was based on the rheostat setting. In general, the rheostat was adjusted to approximately 28 to 30 percent of full voltage (5,600 to 6,000 volts). The voltage applied to the corona, i.e., position of the rheostat, was strongly dependent upon the position of the needle relative to the attractor. When arcing occurred, which was detected both visually and audibly, it was necessary to back off on the rheostat until the arcing just subsided. Current output was extremely low if arcing occurred either continuously or periodically.
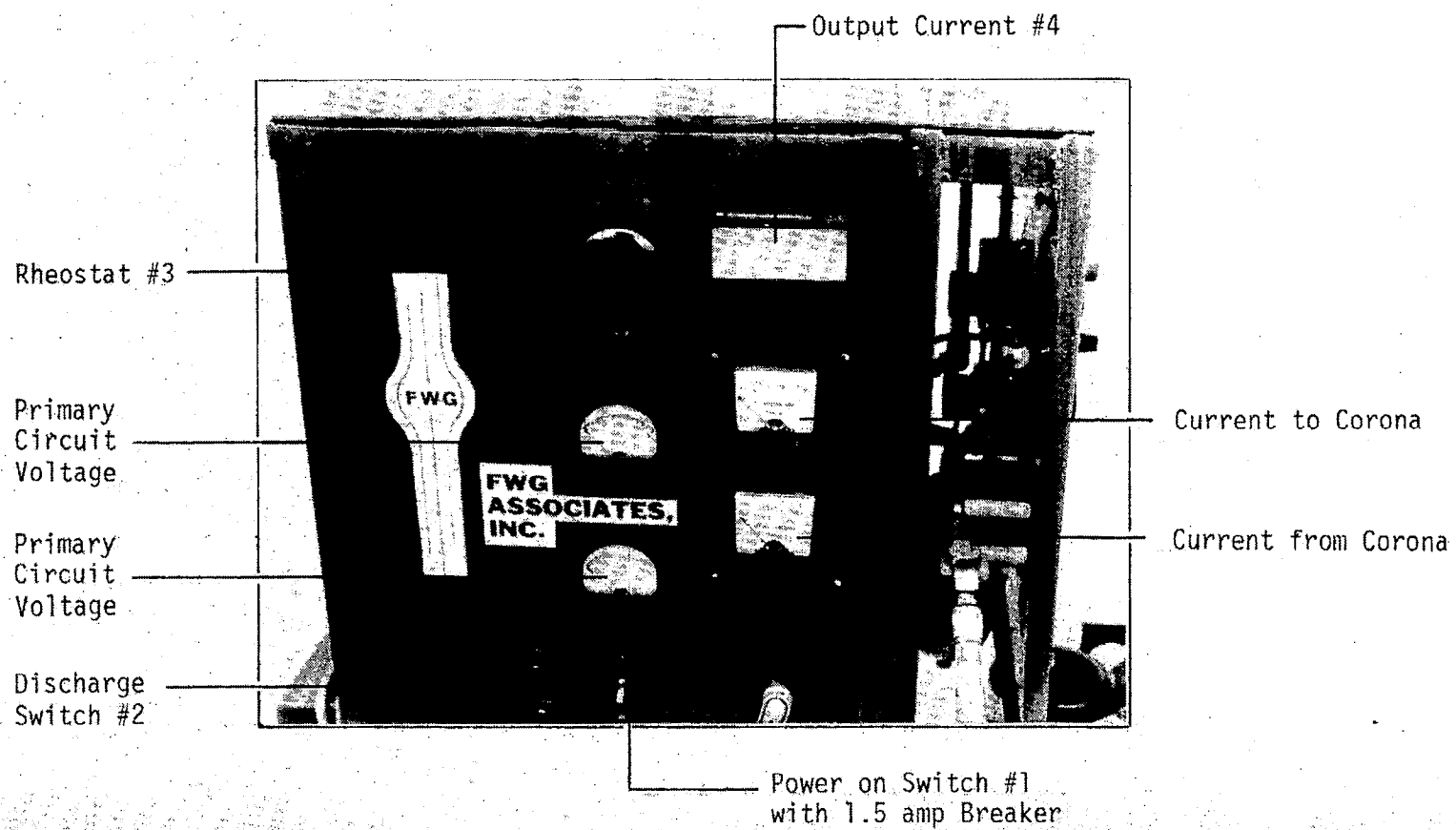
Figure 2.10 Electrical circuit control panel.

3.0 RESULTS AND DISCUSSION

In this section, results of the various tests are discussed. Section 3.1 addresses some of the qualitative observations, in particular the visual glow and arcing observed during testing at night, and Section 3.2 discusses numerical values of the data which have been computed and plotted to illustrate trends.

3.1 Qualitative Observations

Arcing was frequently observed during operation of the charged particle generator. This normally occurred between the needle and the attractor but some times the arc ran along the walls of the nozzle to ground. When arcing occurred, the current output of the system would immediately drop off. Moreover, this seemed to have a hysteresis effect because often once arcing had occurred for any length of time, the high current output which had been achieved prior to arcing was difficult to re-establish. It was also observed that once arcing occurred, it was difficult to eliminate without disassembling the unit and realigning the needle with respect to the nozzle walls. The needle was never visually eroded when inspected after arcing.

During initial tests of the charged particle generator and before experience relative to the behavior of the corona was obtained, a strong arc was often struck and maintained. Luminous particles were then observed to spew out from the nozzle reaching heights of 16 to 20 ft. The physical nature of these luminous particles has not been determined. If a screen apparatus was held in the flow, the particles were observed to bounce off the screen. In turn, they also bounced off the needle arrangement used to measure the output current. It has been suggested that the luminous particles were associated with erosion of the copper

attractor since with strong arcing a greenish-blue glow was observed in the corona region. The present researcher does not believe, however, that this was the case since if it was, the rate of particles issuing from the nozzle was substantial enough to drastically pit the copper attractor. This would result in a continuous change in the corona behavior, which was not observed. Unfortunately, the copper attractors cannot be removed from the nozzle and inspected for pitting to verify this belief.

Under steady operating conditions with the corona properly established, a blue glow was clearly visible in the corona region. A blue glow was also observed issuing from the needle used to measure current output. The blue glow from the needle appeared as a rocket plume diverging from the point of the needle and fanning out into the nozzle exit hole. It is believed, however, that the blue glow was in fact the electrical charged ions or electrons issuing from the nozzle and collecting on the point of the outside needle.

During one run when a light fog existed, static electric effects were felt on the researchers hair when they approached the jet. Also, during damp conditions, a relatively sharp electric shock was experienced if one touched the jet. Under dry conditions, however, these effects were not observed. No noticeable effect on the fog was observed. The fog intensity was so light, however, that one would not expect to see visibility improvement with the unaided eye.

It was also observed that if one closed the water valve and allowed the system to decrease from a high current of approximately 20 μa, the output current slowly decreased but periodically surged upward. This was obviously associated with blowing out of trapped water in the system. When all water deposits had been purged by the dry air, the current would reach a steady value of roughly 2 to 3 μa. This was the same magnitude of current associated with operations when the system power was turned on during start-up before turning on the water injection.

3.2 Current Output

The following sections describe the influence of various experimentally controlled parameters on the current output from the charged particle generator.

3.2.1 Liquid Water Flow Rate

The current output varied with total flow of liquid water as shown in Figure 3.1. In this figure, the current output times the relative humidity, RH (%), of the surrounding atmosphere divided by the stagnation pressure, P_o, correlate very well with the mass flow rate as shown. The scaling parameters RH and P_o were chosen mostly by inspection; however, corona current is well known to scale inversely with pressure (Oglesby and Nichols 1978). Physically, RH is a scale parameter since the higher the humidity the higher the conductivity of the air, and more charge will escape to ground through the air than through the needle.

The optimum current output occurs at a liquid water flow rate in the range of 4 to 6.5 cc/min. The water flowing into the airstream was atomized with a needle valve arrangement as illustrated in Figure 3.2. Air flowing through the 1/4-in tubing shears off the water forming droplets. The initial procedure to estimate the size of the water drops assumed droplets would form having a size of the order of the slot thickness between the needle and its conical seat. It was initially reported (Frost 1981) that the droplet size was highly critical to system performance. Adjusting the needle valve, however, showed that the output current from the system was insensitive to the needle valve opening, which was originally thought to influence the atomization of the water. An experiment was conducted where the needle valve was continuously open during a run with all other parameters held constant. No change in the current output was observed. This observation suggests that the liquid water entering through the needle valve is vaporized with droplets reforming due to condensation in the nozzle. Thus, the author believes that condensation in the nozzle controls the droplet formation and the output current depends only on the magnitude of the water flow rate.
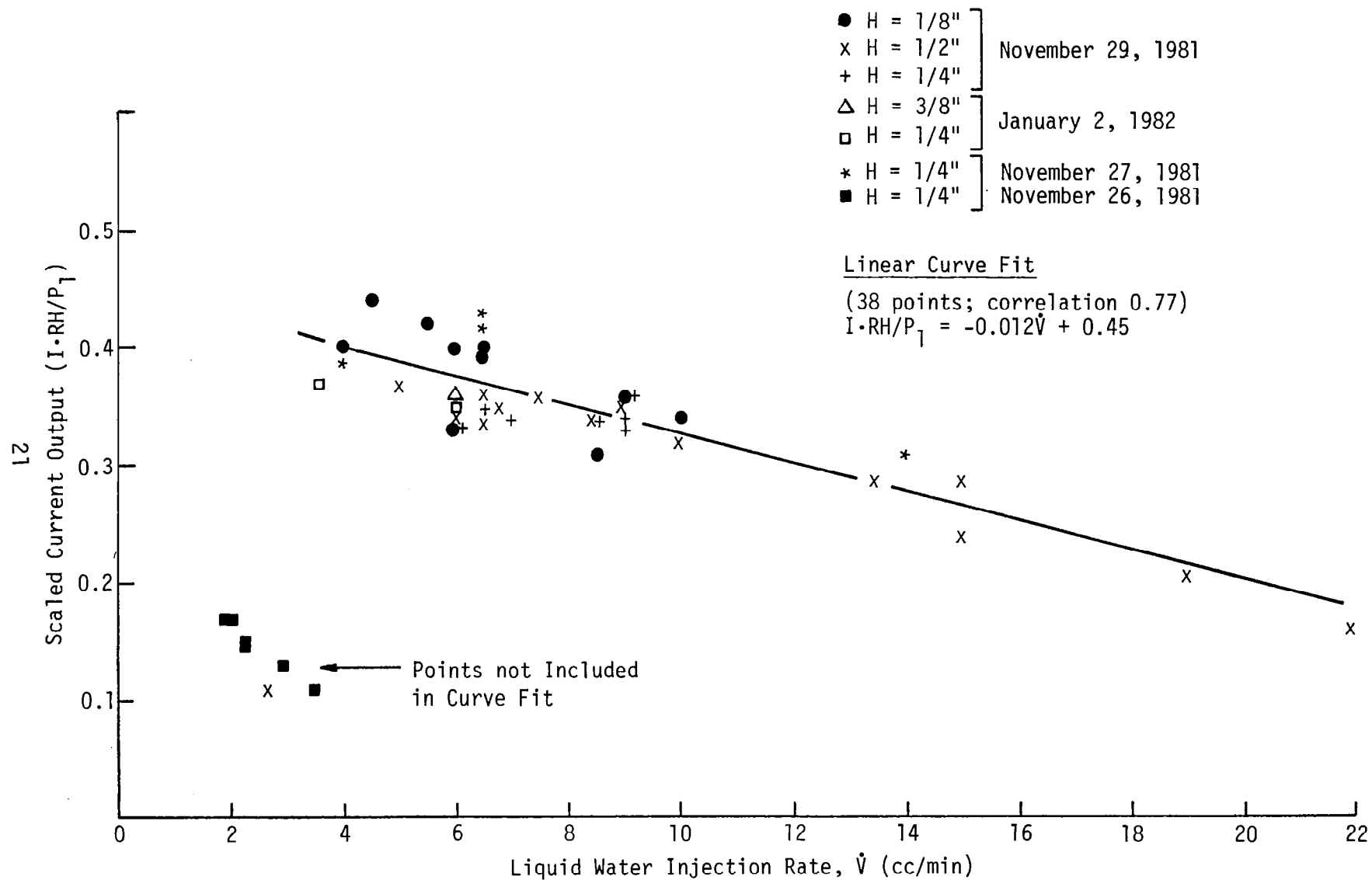
Figure 3.1 Variation of scaled current output with liquid water flow rate.

21
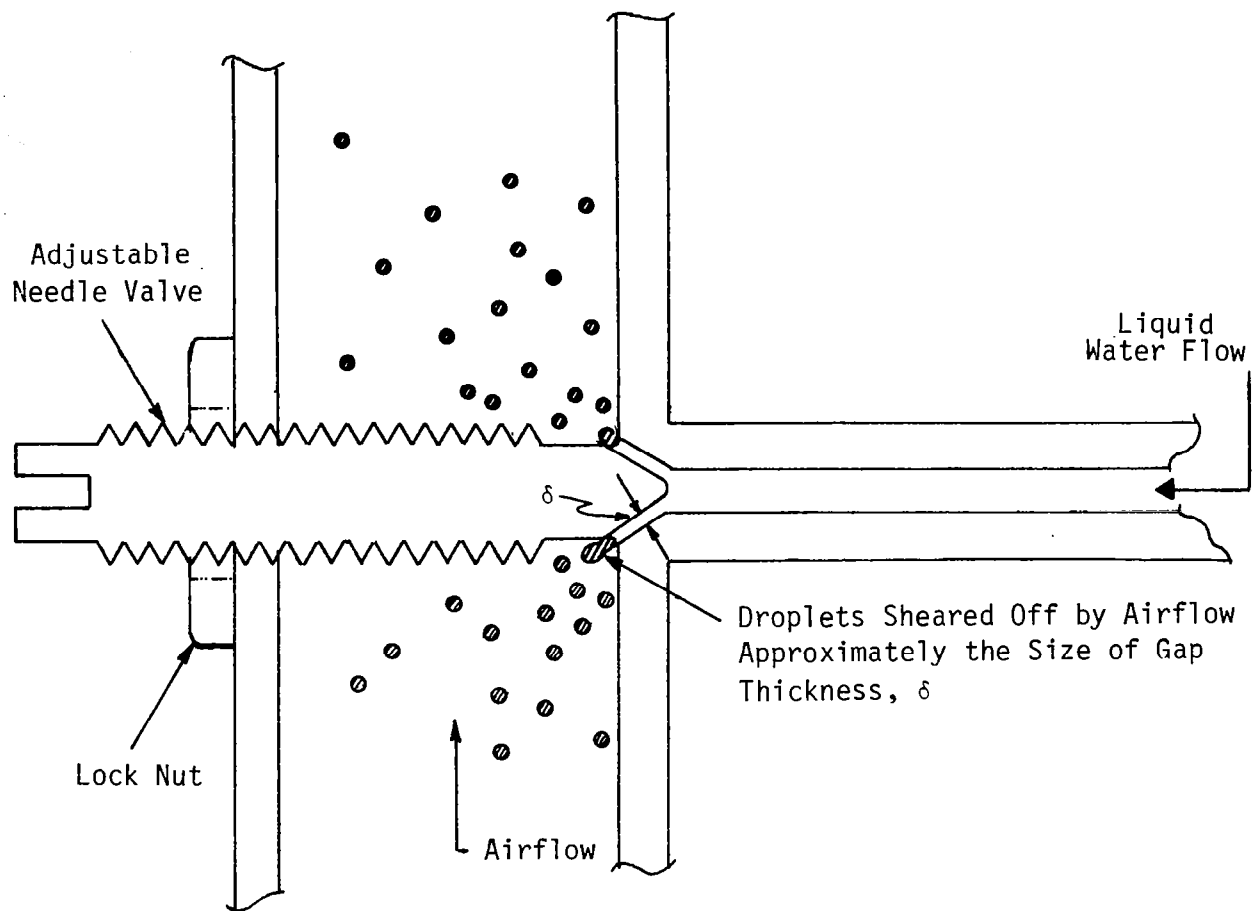
Figure 3.2   Schematic of needle valve atomizer.

Based on choked flow conditions in the nozzle and assuming 6 cc/min of water injected into the airflow stream, the humidity of the air entering the nozzle under optimum current output is computed to increase by approximately 3 percent. The relative humidity of the atmospheric air ranged between 77 to 99 percent. However, how much this was changed after passing through the compressor is unknown.

Although a reasonably good correlation is achieved with liquid water flow rate and current output, the method of controlling the liquid water flow was poor. Since the needle valve had little influence on system performance, the valve on the rotameter became the liquid water flow control. In general, the flow rate dropped off steadily with time

and it was necessary to continuously adjust the rotameter valve. On occasion, however, the flow rate would change suddenly when the cut-in valve on the air compressor would activate. To fully investigate the effects of mass flow rate and to optimize the performance of the system, an automatic control on the water supply is needed along with an accumulator in the air supply circuit. An alternate procedure to achieving a steady flow of liquid water is to isolate the water flow system from the air supply and use a positive displacement precision flow control pump to inject the water. These modifications are being investigated.

3.2.2 Corona Voltage

The method of establishing a corona in the nozzle was very critical to the current output. For most runs, the rheostat was set at approximately 28 percent of full output. This corresponds to roughly 5,600 volts. If an arc or sparking once occurred while bringing up the corona voltage, the current output was considerably reduced even though the voltage was again reduced and the arcing eliminated.

The position of the needle relative to the attractor was extremely critical to whether arcing occurred. A needle length measured as shown in Figure 3.3 (see also Figure 2.4) of 1-15/16 to 1-7/8 inches gave the highest measured current output obtained (approximately 22 μa) with the lower attractor. It was also critical to center the needle relative to
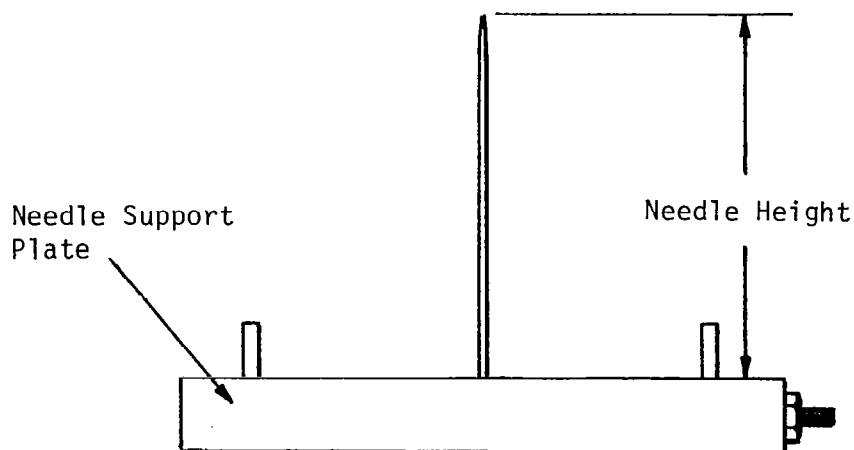
Figure 3.3   Definition of needle height.

23

the attractor. An off-centered needle would often vibrate and hence cause arcing by reducing the gap between the needle and the attractor.

Although it was not possible to measure the resistance across the gap with different needle arrangements, a crude measure was determined from the primary voltage measurement. At a rheostat setting of 28 percent, the primary voltage took on different values depending, apparently, on the needle position. For example, if the primary voltage was 38 volts, the output of the system was not nearly as high as if the voltage was 36 volts. This clearly indicated that the resistance across the gap was higher in the former case than in the later case. A plot of the ratio of primary voltage to rheostat settings versus current output is shown in Figure 3.4. The peak performance appears to occur roughly around 1.29.

This represents only a crude measurement of the actual voltage drop across the needle/attractor gap. A direct voltage measurement is

Figure 3.4   Variation in current output with effective measure of electrical resistance of needle/attractor.

desirable. A commercially available voltmeter to measure at least 10,000 volts imposed across the needle and attractor was not available. A circuit for measuring this high voltage directly is being designed and will be employed to assure an accurate measurement of the voltage.

Since the needle position relative to the attractor and, consequently, the resistance between the needle and the attractor is a critical param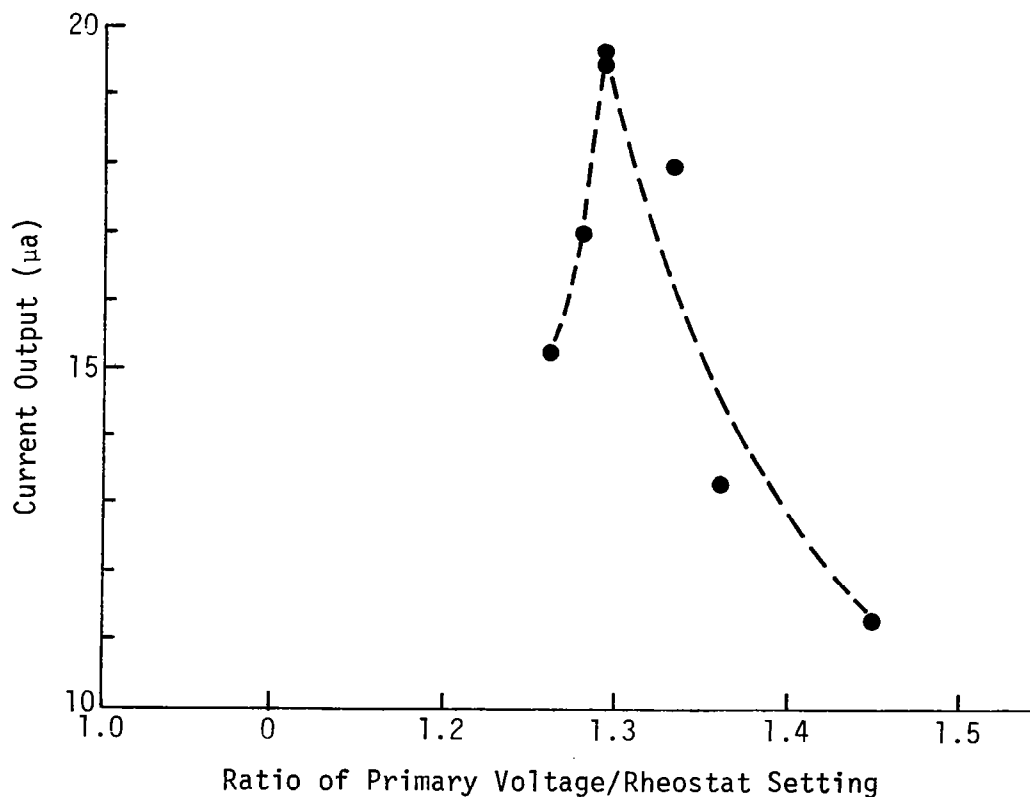eter in the performance of the system, a system modification is required to provide a variable needle position which can be adjusted externally during run conditions. It is proposed that the unit be modified to incorporate external adjustment of the needle. This, however, calls for a major system redesign.

It was also initially planned to measure the current into the needle and the current out of the attractor. Theoretically, the difference between these two currents would represent the current being carried out of the nozzle by the gas jet although it would also include some internal losses. Unfortunately, it was not possible to obtain ammeters which would withstand the high voltage. Three different sets of ammeters were mounted, but all three failed. It was evident that arcing occurred between the needle and the ammeter housing. The cause of this is not clear. The manufacturers concluded that the high voltage caused internal arcing to ground through the ammeter housing. However, the ammeters were, in general, very well insulated being themselves internally insulated and also mounted on Plexiglas which isolated them from a metal framing by at least 4 to 5 inches. Methods of remedying this situation and obtaining an accurate measurement of current into the needle and out of the attractor are being studied.

3.2.3 Corona Needle/Attractor Configuration

In addition to the position of the needle relative to the attractor, different needle configurations were considered. These consisted of a nailhead-type needle and a dual attractor needle as shown in Figure 3.5. Witfall (1968) has observed that a nailhead-type needle provides higher current. However, the nozzle flow system study in the reference was different from the present nozzle. During this investigation, a nailhead-type needle restricted the flow and, consequently, vibrated

25

Standard   Double   Nail
                        Attractor
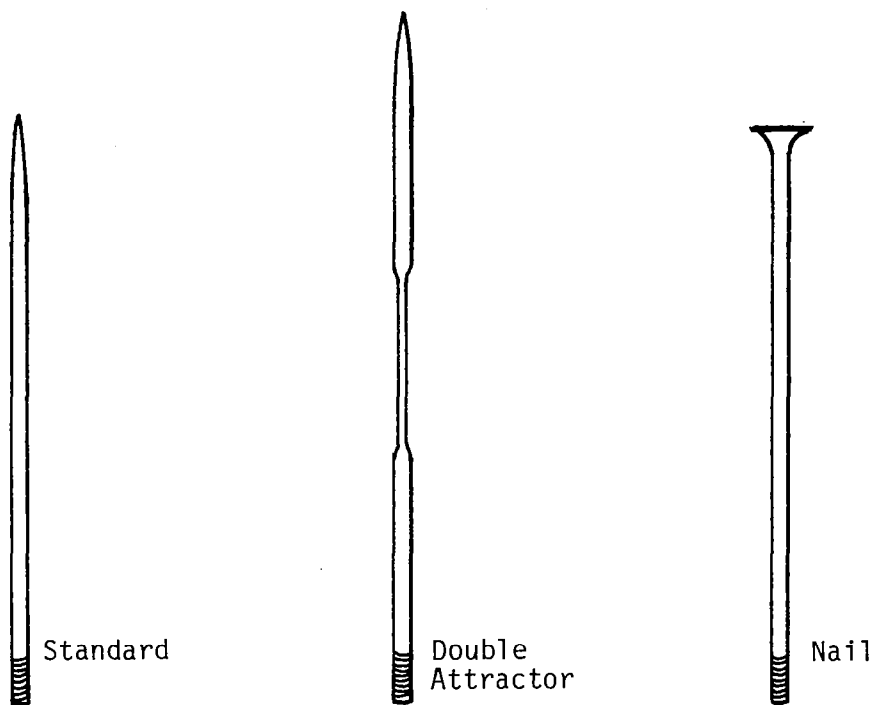
Figure 3.5   Schematic of needle configuration.

strongly producing excessive arcing. No output current above 3 to 4 μa
could be obtained with this arrangement.

Alternately, the double attractor needle, which was designed to
generate a corona at both attractors (see Figure 2.3), also resulted in
considerable arcing. Arcing occurred at the upper part of the needle.
It is possible that shortening the overall length of the needle a frac-
tion of an inch would have provided useful results. Further investiga-
tion of this needle configuration required disassembling the apparatus
and constructing a new needle. A double attractor needle will be inves-
tigated further as time permits.

3.2.4 Pressure

Figure 3.6 shows current output versus nozzle plenum stagnation
pressure. There are two effects associated with varying plenum pressure
and to what extent each impacts this figure is not clear at this time.
One effect is associated with the flow rate through the nozzle. Choked
flow conditions are reached at pressures greater than 16 psia; thus, in

26
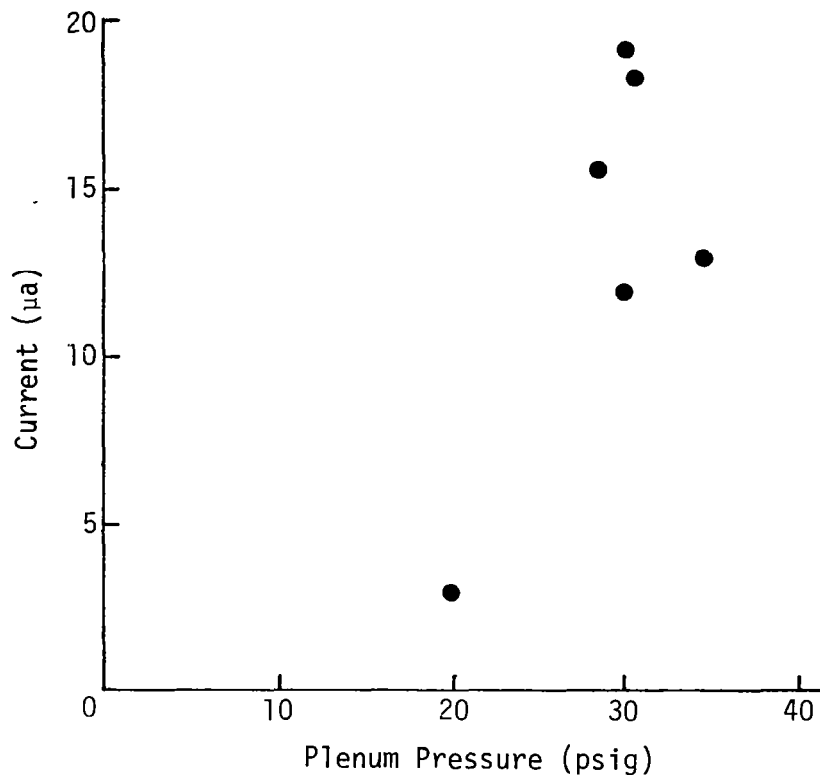
Figure 3.6 Current output variation with plenum pressure.

all cases, choked flow occurs in the nozzle. However, pressure shocks
will occur somewhere along the channel as illustrated schematically in
Figure 3.7 from Owczarek (1964). Under ideal flow conditions, supersonic
flow without disturbances would occur at the nozzle exit. Although the
original design had called for supersonic flow of 1.35 Mach number at
the exit without disturbances, it was necessary to change the needle
size to reduce its vibration in the flow. A change in needle diameter
resulted in a smaller throat area and, consequently, a significant
difference in area ratio which caused appreciably different nozzle flow
characteristics.

The second effect of varying pressure is its influence on the
corona. It is well known that at a given applied voltage, increasing
the pressure of the gas reduces the corona current (Oglesby and Nichols
1978). Since this is normally a monotonic variation, if the effect of
pressure on the output current of the air jet was due to significant
corona variations (output current is assumed to be directly related to
corona current), the curve shown in Figure 3.6 would not have a peak.

a) Variation of pressure in the nozzle.

b) Variation of the Mach number in the nozzle.

Figure 3.7 Performance curves of a convergent/divergent nozzle with
varying ratios of the back pressure to the total pressure
at the inlet. The broken lines denote shock waves
(Owczarek 1964).

Thus, the observed trend in Figure 3.6 is believed to be more closely
associated with the influence of pressure on the flow rate than on the
corona. Further study of this is required.

3.2.5 Spatial Variation of Current in the Air Jet

The variation of output current measured in the air jet was carried
out by adjusting the needle probe vertically and by rotating it to the
various measuring stations illustrated in Figure 2.7. The measured
variation of current with height in the jet is illustrated in Figure
3.8.

The variation of current with height at positions other than on the
centerline are also shown in Figure 3.8. These curves clearly show the
spreading of the charged jet. For example, with the needle at position
#5 (i.e., rotated 180° from the jet) and at a height of 1/4 inch above
the nozzle exit, a current of approximately 5 μa is measured. However,
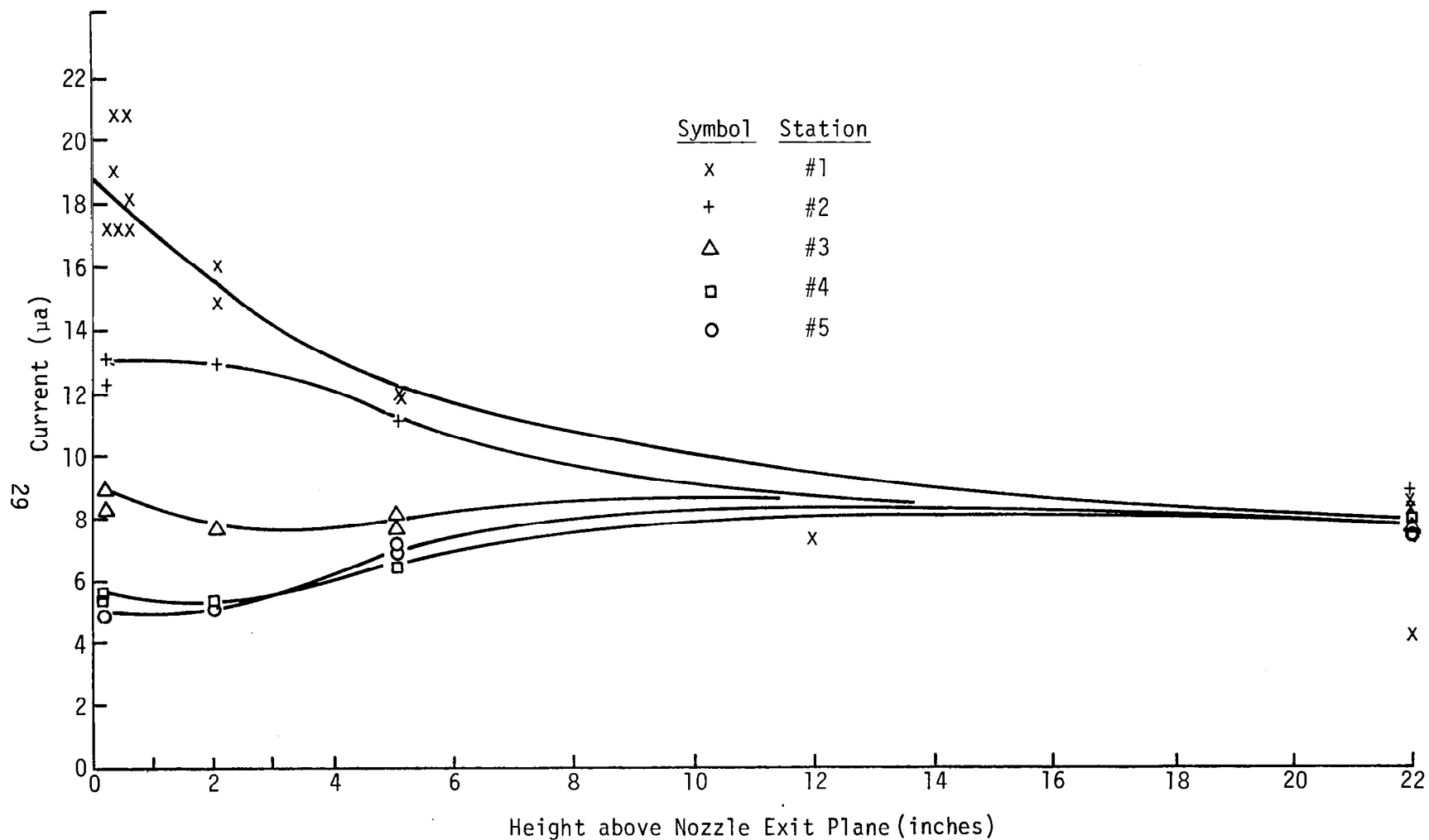as the height of the needle is increased, one sees that the current at

Figure 3.8 Current variation with height in jet (November 29, 1981; January 6, 1982).

position #5 increases and merges with those values at positions closer to the jet centerline ($I \simeq 10$ µa). This shows that the charge in the jet is concentrated at the outlet but fans out becoming more uniformly distributed at greater heights.

It should also be observed from these curves that some charge does flow out the sides of the jet even at positions very close to the nozzle outlet. For example, when the probe is in position #2, which is directly at the edge of the solid portion of the nozzle (see Figure 2.7), a current of approximately 13 µa, 0.68 times the centerline value, is measured. This is believed to be a measure of the charge escaping from the sides of the jet due to the high mobility of the ions.

Figure 3.9 shows the variation of current across the jet at various heights above the nozzle plane. These plots assume that the current is symmetric about the jet centerline and constant along circles drawn through positions #2, #3, #4, and #5. The results shown in this plot are consistent with the expected current profile through a jet (Frost, et al. 1981).

A large enough spatial volume of the jet could not be measured with the present needle arrangement to allow integrating the current over various planes to see whether current is conserved in the jet as is physically required. As noted earlier, the measurement of current with the present needle arrangement does not represent a measure of the total current from the jet. A method of measuring the total current is being investigated. These methods consist of using an induced magnetic flux, a set of reverse polarity plates to collect positive and negative ions separately, or simply a large mesh of copper foil upon which the entire jet would impact. Originally, a screen arrangement was used to capture the charge leaving the jet. This proved unsatisfactory. However, it was later learned that the charged particle generator was not operating efficiently at the time this measurement technique was being used. It is, therefore, necessary to re-evaluate the measurement of current with a plate rather than a needle point.

It should also be noted that any metal object inserted into the charged jet such as the needle distorts the electric field appreciably.
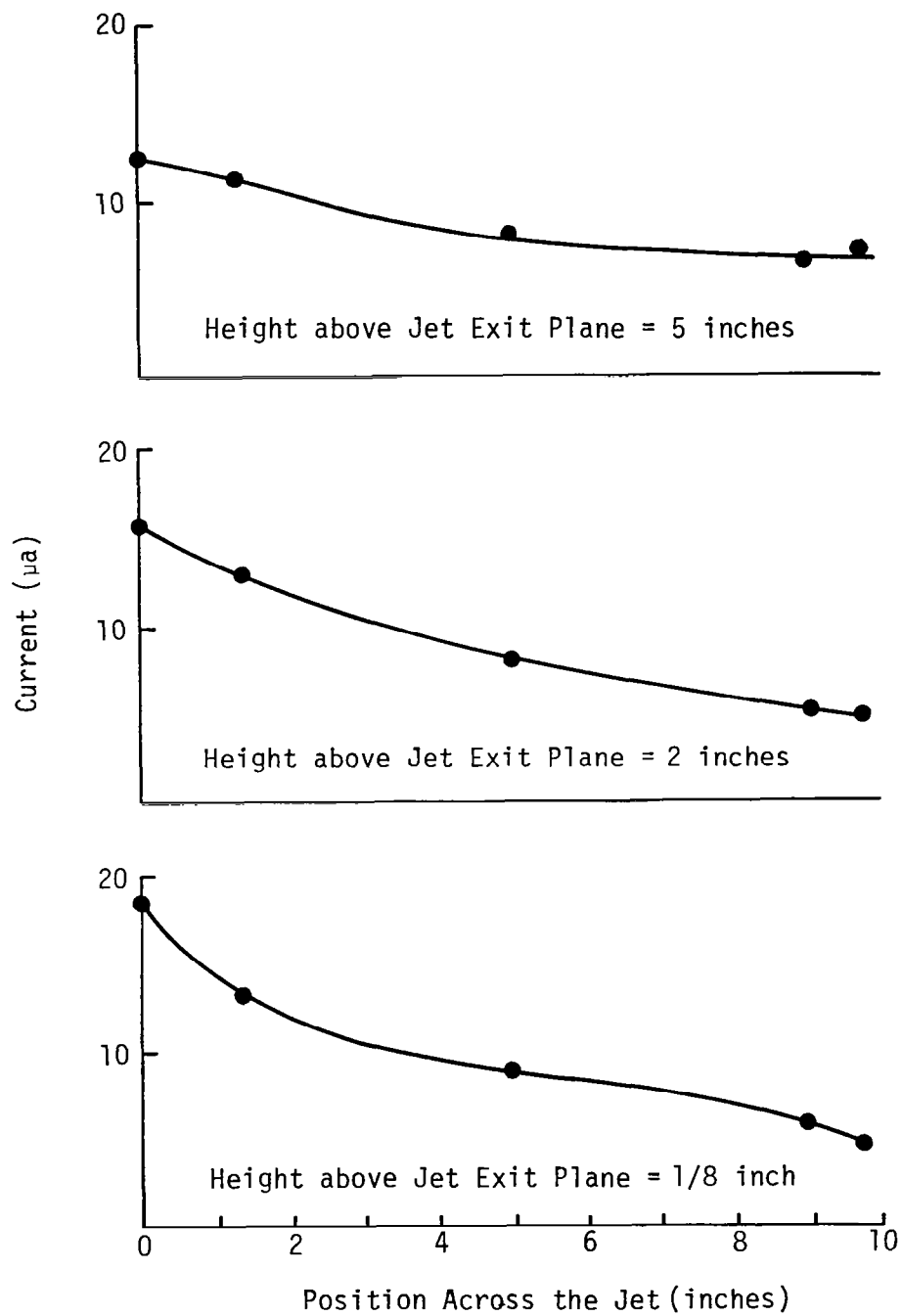
Figure 3.9 Variation of output current across jet (November 29, 1981).

Analyses are being carried out to estimate the magnitude of this distortion. However, the analysis is difficult because the space charge is not uniformly distributed but concentrated in the air jet and drops off rapidly at the edges.

It is also anticipated that the Atmospheric Sciences Division, Marshall Space Flight Center, will, in the near future, have an electric field mill which can be used to measure the electric field in the vicinity of the jet. Once a field mill is available, experiments will be carried out to gain experience on the relationship between the electric field and the air-to-ground current measured with the needle. It should be noted, however, that for an individual charged particle generator the electric field will be highly localized particularly in the jet and difficult to measure with the standard field mill. The electric field of ultimate interest is that which can be created on the scale of an airfield in dimension. This can only be produced with a large grid of several charged particle generators. The resulting overall field could be meaningfully measured with a conventional field mill.

4.0 CONCLUSIONS

The results of the experiments carried out with the prototype charged particle generator have clearly demonstrated that an output current as high as 20 μa measured 1/8 inch above the exit of the nozzle can be routinely achieved with this system. This measurement of current does not necessarily represent the total current but is simply a performance parameter. Although the present unit requires several engineering modifications to be an operational unit, confidence has been achieved from the preliminary results that a charged particle generator which will operate continuously and consistently can be designed and constructed. This is extremely important in determining the direction of the next phase in the investigation of electrical fog dispersal techniques.

One cannot expect that a single unit will disperse fog to a perceptible degree. The charge introduced into a fog by a single unit will be moved around by turbulence and its effect readily diffused. It is well documented (Clark, et al. 1977; Chiang, et al. 1973; Christensen and Frost 1980) that to clear fog on a scale which would benefit aircraft in the terminal area or the transit of ships through the Panama Canal requires a large array of charged particle generators. To prove the ability to disperse fog, a field test is required. The field test carried out by Chiang, et al. (1973) and Clark, et al. (1977) using 16 electrogasdynamic generators similar to the unit described in this report, left many arguments both pro and con relative to the degree of success achieved in dispersing fog.

It is estimated that a field program will require 50 to 100 operational-type charged particle generators (Christensen and Frost 1980; Chiang, et al. 1973). During such a test the researchers cannot spend time with operating the charged particle units. Therefore, prior to going to a large field program, the charge particle generators must be well beyond the experimental stage. Work is required to produce a

charged particle generator which is automated, highly reliable, provides a consistent charge, and requires minimum attention from the operator. Moreover, due to the number of units required, methods of mass producing these economically must be researched.

The results of the present experiment indicate that charged particle generators can produce a current of approximately 20 µa under various atmospheric conditions. A well-defined jet, however, was measurable only to roughly 10 ft above the ground. The dispersion of charge by turbulence to greater heights is hypothesized but can only be proven when an array of units is operated. With an array, the charge will be uniform over a given region and not carried randomly about by one turbulent eddy. The initial prototype is highly research oriented and requires a number of significant design modifications not only to make the unit more operational oriented but also to optimize its performance. Considerable design criteria and insight into the next generation charged particle generator has been gained from this study; however, still more information can be achieved by making minor modifications to the existing research generator. These modifications consist of:

1. Molding a new nozzle with the attractor in the throat and with a correct throat size to allow a 1/16-in needle.

2. Providing means of more precisely controlling the water flow rate and to measure it continuously along with the current output. Water flow rate appears to be the most critical variable affecting charge output.

3. Building or locating commercially available instruments that will stand the high voltage and can be used to measure the current into and out of the corona region as well as the voltage drop across the needle.

4. Establishing methods of measuring the humidity of the air entering the nozzle.

With these modifications, experiments can be carried out to carefully define needed design criteria for the next generation of charged particle generators.

34

With knowledge in hand from the present study, which will be further amplified by the proposed modifications to the existing unit, two directions can be taken in the development of the fog dispersal charged particle generator. One is now to develop a semi-production type generator which is automated. This will demonstrate that multi-units all having equivalent performance (i.e., quality control) in a given field test can be produced in the number required.

Simultaneously, further investigation to optimize the charged particle generator can be carried out by developing a highly research-oriented unit. This unit would be very useful to optimize the performance capability of the generator.

The operational type particle generator should be built and tested to assure the technology to build operational units with at least the capability demonstrated by the preliminary prototype generator reported herein can be mass produced. Although this may not be the optimum design in terms of performance, it is a design which will provide reliable operational units for use in a field test. A field test is necessary to prove whether fog dispersal with electrically charged particles sprayed in at ground level is viable.

Simultaneously, experimental type generators should be developed to further understand the mechanism of the charged particle generator and how the charged particles interact with the fog. These research-type units should have extreme flexibility of configuration, geometrical dimensions, etc.; for example, adjustable nozzle size, remotely controlled needle/attractor positioning, humidity controls, view ports to observe droplets prior to the nozzle plenum chamber, and other such features——the resulting goal being to improve the efficiency and performance of the system.

REFERENCES

Chapman, S.: Electrostatic Field Measurements, Corona Discharge and Thunderclouds, CAL Report 68, Cornell Aeronautical Lab., Buffalo, N.Y., 1956.

Chiang, T. K., Wright, T., and Clark, R.: Field Evaluation of an Electrogasdynamic Fog Dispersal Concept, FAA Report FAA-RD-73-33, Department of Transportation, Federal Aviation Administration, Washington, D.C., 1973.

Christensen, Larry S., and Frost, Walter: Fog Dispersion, NASA CR 3255, 1980.

Clark, R. S., Wright, T. L., Evert, R. W., Loveland, R. B., Northrup, R. E., Jr.: Project Foggy Cloud V Panama Canal Warm Fog Dispersal Program, Report No. NWC TP 5542, Naval Weapons Center, China Lake, California, 1977.

Collins, Frank G., Frost, Walter, and Kessel, Philip: Design of Prototype Charged Particle Fog Dispersal Unit, NASA CR 3481, 1981.

Davis, R., and Standring, W. G.: Discharge Currents Associated with Kite Balloons, Proc. Roy. Soc. A, 191:304-322, 1947.

Frost, Walter: Monthly Progress Report for Warm Fog Dissipation Program, Contract NAS8-33541, Reporting Period October 13 - November 13, 1981.

Frost, Walter, Collins, Frank G., and Koepf, David: Charged Particle Concepts for Fog Dispersion, NASA CR 3440, 1981.

Harris, D. J.: Atmospheric Electric Field Measurements During the Harmattan Dust Haze in Northern Nigeria, Planetary Electrodynamics (Coroniti, S. C., and Hughes, J., editors), Vol. I. New York: Gordon and Breach Science Publishers, pp. 39-47, 1969.

Kolokolov, V. P., and Lobodin, T. V.: Studies in Atmospheric Electricity. Translated from Russian by Israel Program for Scientific Translations, Jeruselum, 1974.

Marks, Alvin M., and Kent, Arthur P.: Wind Power Charged Aerosol Generator, Final Technical Summary for the period September 27, 1977 to September 26, 1978, Report COO/2774/77-1 UC-60, U. S. Department of Energy, 1979.

Mason, B. J.: The Physics of Clouds. New York: Oxford University Press, 1971.

Oglesby, Sabert, Jr., and Nichols, Grady B.: Electrostatic Precipitation. New York: Marcel Dekker, Inc., 1978.

Owczarek, Jerzy A.: Fundamentals of Gas Dynamics. Scranton, Penn.: International Textbook Company, 1964.

Simpson, G. C., and Robinson, G. D: The Distribution of Electricity in Thunderclouds II, Proc. Roy. Soc. A, 177:281-329, 1940.

Simpson, G. C., and Scarse, F. J.: The Distribution of Electricity in Thunderclouds, Proc. Roy. Soc. A, 161:309-352, 1937.

Whipple, F. J. W., and Scarse, F. J.: Point Discharge in the Electric Field of the Earth, Geophys. Mem., London, 68:1-20, 1936.

Wifall, James R.: Effects of Electrode Geometry-Similarity and Scaling Laws in EFD Energy Conversion Processes, II. Experimental Results, AGARDograph 122, Selected Topics in Electrofluid Dynamic Energy Conversion, 1968.

Willke, Theodore L.: Current Production in a Cylindrical Geometry Electrofluid Dynamic Generator, Report ARL 71-0245, Air Force Systems Command, 1971.

1. REPORT NO. NASA CR-3654	2. GOVERNMENT ACCESSION NO.	3. RECIPIENT'S CATALOG NO.
4. TITLE AND SUBTITLE Preliminary Test Results of Electrical Charged Particle Generator for Application to Fog Dispersal		5. REPORT DATE November 1982
		6. PERFORMING ORGANIZATION CODE
7. AUTHOR(S) Walter Frost		8. PERFORMING ORGANIZATION REPORT #
9. PERFORMING ORGANIZATION NAME AND ADDRESS FWG Associates, Inc. R.R. 2, Box 271-A Lakewood Drive Tullahoma, TN 37388		10. WORK UNIT NO. M-394
		11. CONTRACT OR GRANT NO. NAS8-33541, Ext. No. 1
12. SPONSORING AGENCY NAME AND ADDRESS National Aeronautics and Space Administration Washington, D.C. 20546		13. TYPE OF REPORT & PERIOD COVERED Contractor Report
		14. SPONSORING AGENCY CODE

15. SUPPLEMENTARY NOTES

Prepared for: Space Science Laboratory, Atmospheric Sciences Division
Marshall Technical Monitor: Dennis Camp
Final Report

16. ABSTRACT

A charged particle generator for use in fog dispersal applications was built and preliminary tests were carried out. The parameter used as a measure of performance was the current measured with a needle probe positioned in the charged jet connected to ground through an ammeter. The needle was movable and allowed the current profile throughout the jet to be determined. The measured current is referred to as the "current output." The major independent parameters were liquid water injection rate, plenum pressure, and corona voltage. Optimum current output was achieved at the approximate pressure of 30 psig, corona voltage of 5600 volts, and liquid water injection rate of 6 cc/min.

The results of the test with the prototype charged particle generator clearly demonstrate that a current on the order of 20 µa can be routinely achieved with the system. This measurement of current does not necessarily represent the total issuing from the nozzle current which is expected to be larger. From these results, confidence has been established that a charged particle generator which will operate continuously and consistently can be designed, constructed, and operated. Further work is required, however, to better understand the physical mechanisms involved and to optimize the system for fog dispersal application.

17. KEY WORDS Charged Particle Generator Visibility Fog Dispersal	18. DISTRIBUTION STATEMENT Unclassified - Unlimited Subject Category 47

19. SECURITY CLASSIF. (of this report) Unclassified	20. SECURITY CLASSIF. (of this page) Unclassified	21. NO. OF PAGES 46	22. PRICE A03